Computed torque control of two-stage Gough-Stewart platform in oscillation generation and balance stabilization applications

Ha Huy Hung [1], Hoang Quang Chinh [1]
[1]Le Quy Don Technical University, Ha Noi, Viet Nam.
Corresponding Author: Ha Huy Hung

ABSTRACT : *This study focuses on a two-stage Gough-Stewart platform. The lower stage generates the oscillatory motions of ships on sea, while the upper stage is equipped to stabilize or control motion with trajectory tracking capabilities. The dynamic model of the robotic system is formulated using the Lagrange equations. Based on this model, a computed torque controller is developed in task space. Oscillation generation and stabilization are evaluated through simulations utilizing the kinematic and dynamic parameters of two Bosch Rexroth robots. The simulation results confirm the precision of the dynamic model and the efficiency of the designed controller.*
KEYWORDS *Gough-Stewart platform, parallel robots, Dynamics, PD control.*

I.   INTRODUCTION

The robot system includes two Gough-Stewart platforms (GSPs) [1] arranged in lower and upper stages. Each GSP consists of an upper work plate and a lower base plate, connected by six legs with universal joints. The length of these legs is controlled by either electric motors or hydraulic cylinders. As shown in Figure 1, the lower stage of the two-stage GSP generates oscillations, while the upper stage is dedicated to stability maintenance. Sensors on the work plates of both stages provide direct measurements of the plates' position, orientation, velocity, and angular velocity.
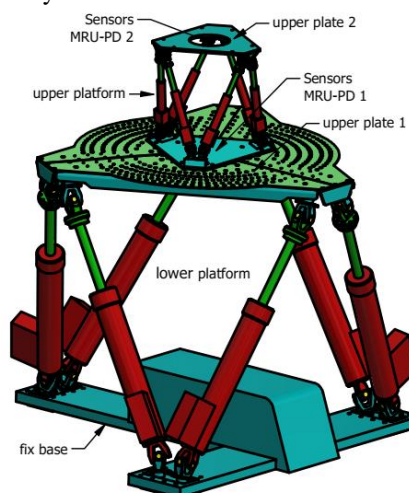

Fig. 1. Design of the 2-dof balancing table

The GSP's high rigid structure and precise positioning make it valuable across numerous applications, including flight simulation, robotic surgery, precision machining, and mobile stabilization. Balance stabilization is essential for various equipment on transportation vehicles, such as cooking tables, treatment tables, and gangways on ships [2,3]. By using the GSP to generate the oscillations of moving vehicles, a semi-natural simulation system for motion or balance stabilization control is achieved. This approach mitigates the high

costs, time, and complexity involved in performing motion stability control research directly on diverse mobile platforms across different vehicle types and terrains.

Many researchs have addressed the dynamics modeling and control of GSP, utilizing motion equations like Newton-Euler, Lagrange, Kane's equations, or principles of virtual work [4-6]. Control methods have been applied to GSP, including kinematic control, inverse dynamics in joint and task space, PID, sliding mode, adaptive controls and others [7-9]. While single-stage GSP are frequently studied, research on multi-stage GSPs remains limited due to the challenges of their closed-chain mechanisms and high degrees of freedom [8-13].

This paper develops a dynamic model and computed torque controller for a two-stage GSP, employing a multibody approach based on Lagrange's equations with multipliers. The structure of the paper is as follows: Section 1 provides an introduction; Section 2 details the kinematic and dynamic modeling of the two-stage GSP; Section 3 presents the controller design; Section 4 describes the parameters of the robot system used in simulation; Section 5 presents comptation and simulation; Section 6 discusses the results and concludes the paper.

II. DERIVING KINEMATIC AND DYNAMIC EQUATIONS

To establish the kinematic equations for the two-stage GSP, the coordinate frames are assigned to the robot's links. Figure 2a illustrates the kinematic diagram of the complete two-stage GSP, while Figure 2b depicts the kinematic layout of a single GSP at the k-th stage, where k=1,2.
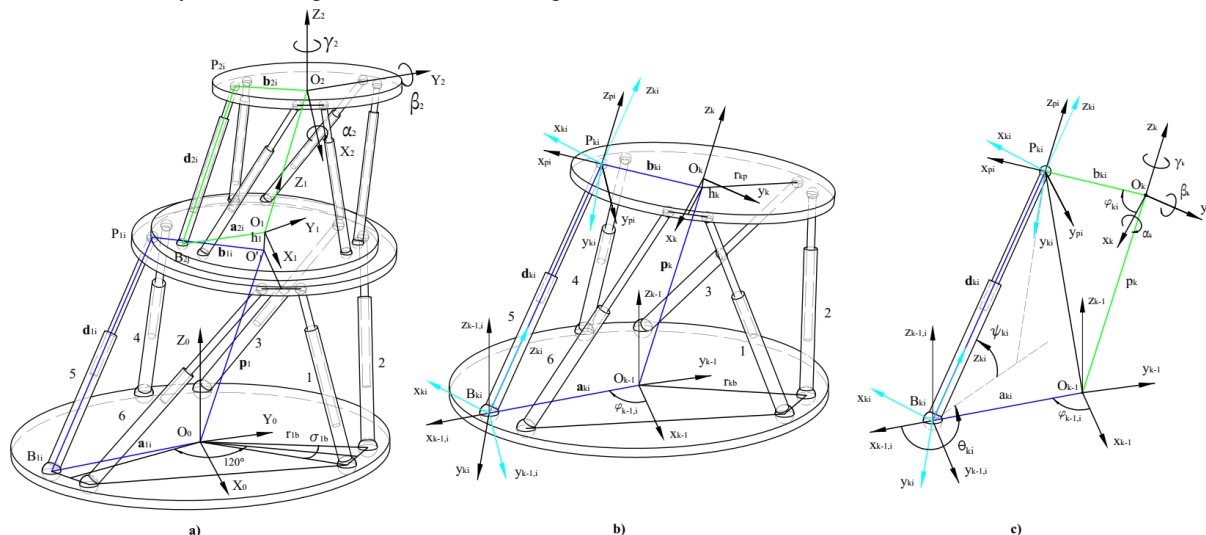
Fig. 2. The two-stage Gough-Stewart platforms

Notations: B_k is the base plate, P_k. is the work plate of the k-th platform. B_{ki}, P_{ki} is the center of the joints on the B_k, P_k (i=1..6), respectively.

The base frame $O_0x_0y_0z_0$ is attached at the center of the base plate of the lower platform, with the z_0 axis perpendicular to the plate B_k and pointing upwards, and the x_0 axis passing through the midpoint of the line connecting joints B_{k1} and B_{k6}. The frames $O_kx_ky_kz_k$ (k=1,2) are attached to the work plates of the corresponding platform at stage 1 and stage 2, where the z_k axis is perpendicular to the plate P_k and points upwards, and the x_k passes through the midpoint of the line connecting joints P_{k1} and P_{k6}. The distance from the center of the plates to the joint centers on the corresponding plates are a_{1i}, b_{1i}, a_{2i}, b_{2j}, respectively. The leg lengths of the robots at levels 1 and 2 are denoted as d_{1i}, d_{2j}, where i, j = 1,..,6.

The frame $B_{ki}x_{k-1,i}y_{k-1,i}z_{k-1,i}$ is attached to the base plate (lower plate), with the origin at the center of the i-th joint; the axis $B_{ki}x_{k-1}$ coincides with $O_{k-1}B_{ki}$; the axis $B_{ki}z_{k-1,i}$ is perpendicular to the plane of the base plate and points upwards. The frame $P_{ki}x_{pi}y_{pi}z_{pi}$ is attached to the plate P_k, with the origin at the center of the i-th joint; the axis $P_{ki}x_{pi}$ coincides with O_kP_{ki}; the axis $P_{ki}z_{pi}$ is perpendicular to the plate P_k.

The generalized coordinate vectors, which define the orientation and position in the workspace of the work plates of robots 1 and 2, are denoted as $\mathbf{p}_1$, $\mathbf{p}_2$, respectively:

$$\mathbf{p}_k = \begin{bmatrix} x_k & y_k & z_k & \alpha_k & \beta_k & \gamma_k \end{bmatrix}^T, \ k = 1, 2 \tag{1}$$

The generalized coordinate vectors in the joint space of the robots 1 and 2 is:

$$\mathbf{q}_k = \begin{bmatrix} \mathbf{d}_k & \boldsymbol{\theta}_k & \boldsymbol{\psi}_k \end{bmatrix}^T, \ k = 1, 2 \tag{2}$$

Where $\mathbf{d}_k, \boldsymbol{\theta}_k, \boldsymbol{\psi}_k$ is the generalized coordinate vectors with components being the lengths and angles of the legs of the lower and upper platform, respectively.

$$\mathbf{d}_k = \begin{bmatrix} d_{k1} & d_{k2} & d_{k3} & d_{k4} & d_{k5} & d_{k6} \end{bmatrix}^T$$

$$\boldsymbol{\theta}_k = \begin{bmatrix} \theta_{k1} & \theta_{k2} & \theta_{k3} & \theta_{k4} & \theta_{k5} & \theta_{k6} \end{bmatrix}^T, \; k = 1, 2 \tag{3}$$

$$\boldsymbol{\psi}_k = \begin{bmatrix} \psi_{k1} & \psi_{k2} & \psi_{k3} & \psi_{k4} & \psi_{k5} & \psi_{k6} \end{bmatrix}^T$$

Consider the kinematic loop of the i-th leg at stage k of the robot, as shown in Figure 3. The coordinates of point P in the O_{k-1} frame is determined in two ways, corresponding to two paths. The transformation from the frame $O_{k-1}x_{k-1}y_{k-1}z_{k-1}$ to the frame $P_{ki}x_{ki}y_{ki}z_{k}i$ through the two paths is as follows:

Path 1: Rotate the frame $O_{k-1}x_{k-1}y_{k-1}z_{k-1}$ around the z_{k-1} axis by an angle φ_{ki}, then translate along the $x_{k-1,i}$ axis by a distance r_{kb}. Rotate the frame $B_{ki}x_{k-1,i}y_{k-1,i}z_{k-1,i}$ around the $B_{ki}x_{k-1,i}$, $B_{ki}y_{k-1,i}$, axes by the angles θ_{ki}, ψ_{ki}. Translate $B_{ki}x_{ki}y_{ki}z_{ki}$ along the z_{ki} axis by a distance d_{ki}.

Path 2: Perform three basic rotations by angles α_k, β_k, γ_k and three basic translations along the x_{k-1}, y_{k-1}, z_{k-1} axes to take the frame $O_{k-1}x_{k-1}y_{k-1}z_{k-1}$ into alignment with the frame $O_kx_ky_kz_k$. Rotate the frame $O_kx_ky_kz_k$ around the z_k axis by an angle φ_{ki}, then translate along the x_k axis by a distance r_{kb}.

Following the two kinematic paths at the i-th leg, by determining the homogeneous transformation matrices at each step and multiplying the transformation matrices together, we obtain the homogeneous matrices that determine the position and orientation of the frame $P_{ki}x_{ki}y_{ki}z_{ki}$ relative to the frame $O_{k-1}x_{k-1}y_{k-1}z_{k-1}$ as follows:

$$^{k-1}\mathbf{A}_{1,ki} = {}^{k-1}\mathbf{A}_{k-1,i}\left(r_{kb}, \varphi_{k-1,i} \right) {}^{k-1,i}\mathbf{A}_{ki}\left(\psi_{ki}, \theta_{ki}, d_{ki} \right)$$

$$^{k-1}\mathbf{A}_{2,ki} = {}^{k-1}\mathbf{A}_{k}\left(x_k, y_k, z_k, \alpha_k, \beta_k, \gamma \right) {}^{k}\mathbf{A}_{ki}\left(r_{kp}, \varphi_{ki} \right); \quad k = 1, 2; \; i = \overline{1, 6} \tag{4}$$

From (4), since the position of point P_{ki} calculated from both paths is the same, we obtain three equations based on the position of point P_{ki} as follows:

$$\begin{cases} f_{i1} = {}^{k-1}\mathbf{A}_{1,ki}[1,4] - {}^{k-1}\mathbf{A}_{2,ki}[1,4] \\ f_{i3} = {}^{k-1}\mathbf{A}_{1,ki}[2,4] - {}^{k-1}\mathbf{A}_{2,ki}[2,4] \quad ; i = 1,..,6 \\ f_{i3} = {}^{k-1}\mathbf{A}_{1,ki}[3,4] - {}^{k-1}\mathbf{A}_{2,ki}[3,4] \end{cases} \tag{5}$$

Thus, for each kinematic loop of the i-th leg, we have 3 equations. Since a single platform of the robot has 6 legs, there are a total of 18 equations:

$$\mathbf{f}_k(\mathbf{q}_k) = \mathbf{f}_k(\mathbf{p}_k); \; \mathbf{q}_k = \begin{bmatrix} \psi_{ki}, \theta_{ki}, d_{ki} \end{bmatrix}^T ; \; i = 1,..,6; \; k = 1,2; \mathbf{p}_k = \begin{bmatrix} x_k, y_k, z_k, \alpha_k, \beta_k, \gamma_k \end{bmatrix}^T \tag{6}$$

Equation (6) can be simplified to the following form:

$$\mathbf{f}_k(\mathbf{q}_k, \mathbf{p}_k) = \mathbf{f}_{18x1}(\mathbf{q}_k, \mathbf{p}_k) = \mathbf{f}_k(\mathbf{X}_k) = 0$$

$$\mathbf{X}_k = (\mathbf{q}_k, \mathbf{p}_k); \quad k = 1, 2 \tag{7}$$

Considering both levels of the robot, k=1, 2, we obtain the generalized kinematic equations of the two-stage robot system, consisting of 36 equations.

Kinematic problems: The forward kinematics problem is to determine the position and orientation of the work plate (workspace variables $\mathbf{p}_k$) from the known joint variables (joint space variables $\mathbf{q}_k$ or $\mathbf{d}_k$), at a specific stage of the robot system. The inverse kinematics problem is to compute the variables in the joint space (find $\mathbf{d}_k$, $\mathbf{q}_k$), given the desired motion of the work plate (given $\mathbf{p}_k$).

Velocities computation: The velocities of the rigid bodies (links) in the robot system are generally calculated for the k-th stage of the robot. By differentiating the first equation of equation (6), we obtain:

$$\sum_{i=1}^{18} \frac{\partial \mathbf{f}_{k\xi}}{\partial \mathbf{p}_{ki}} \dot{\mathbf{p}}_{ki} = -\sum_{j=1}^{6} \frac{\partial \mathbf{f}_{k\xi}}{\partial \mathbf{q}_{kj}} \dot{\mathbf{q}}_{kj} \; ; \xi = 1,...,18 \; \Leftrightarrow \; \mathbf{J}_{Pk}\dot{\mathbf{p}}_k = \mathbf{J}_{qk}\dot{\mathbf{q}}_k \tag{8}$$

From (8), the velocities of the generalized coordinates in the joint space can be calculated:

$$\dot{\mathbf{q}}_k = \mathbf{J}_{qk}^{-1}\mathbf{J}_{pk}\dot{\mathbf{p}}_k \tag{9}$$

Accelerations computation:

Differentiate equations (8) with respect to time:

$$\sum_{j=1}^{18}\sum_{i=1}^{18} \frac{\partial^2 \mathbf{f}_{k\xi}}{\partial \mathbf{p}_{ki}\partial \mathbf{p}_{kj}}\dot{\mathbf{p}}_{ki}\dot{\mathbf{p}}_{kj} + \sum_{i=1}^{18} \frac{\partial \mathbf{f}_{k\xi}}{\partial \mathbf{p}_{ki}}\ddot{\mathbf{p}}_{ki} = -\sum_{s=1}^{6}\sum_{l=1}^{6} \frac{\partial^2 \mathbf{f}_{k\xi}}{\partial \mathbf{q}_{ks}\partial \mathbf{q}_{sl}}\dot{\mathbf{q}}_{ks}\dot{\mathbf{q}}_{kl} + \sum_{s=1}^{6} \frac{\partial \mathbf{f}_{k\xi}}{\partial \mathbf{q}_{ks}}\ddot{\mathbf{q}}_{ks} \; , \; \xi = 1,..,18 \tag{10}$$

Equation (10) is rewritten in the following form:

$$\mathbf{J}_{pk}\ddot{\mathbf{p}}_k = \mathbf{g}_k ; \quad \mathbf{g}_k = \begin{bmatrix} \mathbf{g}_{k1}, & \mathbf{g}_{k2}, & . & . & . & \mathbf{g}_{k18} \end{bmatrix}$$

$$\mathbf{g}_{k\xi} = -\sum_{j=1}^{18}\sum_{i=1}^{18}\frac{\partial^2 \mathbf{f}_{k\xi}}{\partial \mathbf{p}_{ki}\partial \mathbf{p}_{kj}}\dot{\mathbf{p}}_{ki}\dot{\mathbf{p}}_{kj} - \sum_{s=1}^{6}\sum_{l=1}^{6}\frac{\partial^2 \mathbf{f}_{k\xi}}{\partial \mathbf{q}_{ks}\partial \mathbf{q}_{sl}}\dot{\mathbf{q}}_{ks}\dot{\mathbf{q}}_{kl} + \sum_{s=1}^{6}\frac{\partial \mathbf{f}_{k\xi}}{\partial \mathbf{q}_{ks}}\ddot{\mathbf{q}}_{ks} , \quad \xi = 1,..,18 \tag{11}$$

Differentiate equation (9) to obtain the acceleration of the generalized coordinates in joint space:

$$\ddot{\mathbf{q}}_k = \mathbf{J}_{qk}^{-1}\mathbf{J}_{pk}\ddot{\mathbf{p}}_k + \mathbf{J}_{qk}^{-1}\dot{\mathbf{J}}_{pk}\dot{\mathbf{p}}_k - \mathbf{J}_{qk}^{-1}\dot{\mathbf{J}}_{qk}\dot{\mathbf{q}}_k \tag{12}$$

Dynamic modeling of the the two-stage GSPs

GSP is derived first; then, the dynamic model of the two-stage GSPs is combined and solved simultaneously.

This section presents the dynamic modeling for the k-th stage of the robot as shown in Fig.1b. The generalized coordinates and the first and second derivatives of the generalized coordinates for the k-th stage of the robot in the dynamic problem include 18 joint variables, represented in the algebraic vector $\mathbf{q}_k$, and 6 generalized coordinate variables of the work plate P_k, represented in the algebraic vector $\mathbf{p}_k$.

Applying the Lagrange equations of motion with Lagrange multipliers, the dynamic state of the k-th stage robot system is described by the constraint equations (6) and the differential equations of motion:

$$\begin{cases} \mathbf{M}_k\left(\mathbf{X}_k\right)\ddot{\mathbf{X}}_k + \mathbf{C}_k\left(\mathbf{X}_k, \dot{\mathbf{X}}_k\right)\dot{\mathbf{X}} + \mathbf{P}_k\left(\mathbf{X}_k\right) + \mathbf{Q}_k\left(\mathbf{X}_k\right) + \mathbf{U}^*_k = \mathbf{U}_k \\ \mathbf{f}_k\left(\mathbf{X}_k\right) = 0, \quad k = 1, 2 \end{cases} \tag{13}$$

Where: $\mathbf{x}_k, \dot{\mathbf{x}}_k, \ddot{\mathbf{x}}_k$ are the generalized coordinate vector, its first and second time derivatives, respectively:

$$\mathbf{X}_k = (\mathbf{q}_k, \mathbf{p}_k); \quad \dot{\mathbf{X}}_k = (\dot{\mathbf{q}}_k, \dot{\mathbf{p}}_k); \quad \ddot{\mathbf{X}}_k = (\ddot{\mathbf{q}}_k, \ddot{\mathbf{p}}_k) \tag{14}$$

$\mathbf{M}_k(\mathbf{X}_k)$ is the generalized mass matrix:

$$\mathbf{M}_k\left(\mathbf{X}_k\right) = \begin{bmatrix} m_{k1,1} & m_{k1,2} & ... & m_{k1,24} \\ ... & ... & ... & ... \\ m_{k24,1} & m_{k24,2} & ... & m_{k24,24} \end{bmatrix} \tag{15}$$

The matrix $\mathbf{M}_k(\mathbf{X}_k)$ is calculated as follows:

$$\mathbf{M}_k\left(\mathbf{X}_k\right) = \sum_{i=1}^{n}\left(m_{ki}\mathbf{J}_{Ti}^T\mathbf{J}_{Ti} + \mathbf{J}_{Ri}^T\mathbf{I}_i\mathbf{J}_{Ri}\right); \quad \mathbf{J}_{Ti} = \frac{\partial \mathbf{r}_{ci}}{\partial \mathbf{X}_k}; \quad \mathbf{J}_{Ri} = \frac{\partial \boldsymbol{\omega}_i}{\partial \mathbf{X}_k} \tag{16}$$

With n being the number of moving links at stage k, m_i is the mass of the i-th moving link. $\mathbf{J}_{Ti}, \mathbf{J}_{Ri}$ are the translational Jacobian matrix and the rotational Jacobian matrix of the i-th moving link. These matrices are calculated based on the position of the center of mass and the angular velocity of the links. $\mathbf{I}_i$ is the inertia tensor of the link with respect to the coordinate system located at the center of mass.

The angular velocity of the i link in the system is calculated using the skew symmetric matrix, through the direction cosine matrix A_i of link i:

$$\tilde{\boldsymbol{\omega}}_i\left(\mathbf{X}_k, \dot{\mathbf{X}}_k\right) = \mathbf{A}_i^T\dot{\mathbf{A}}_i = \begin{bmatrix} 0 & -\omega_{iz} & \omega_{iy} \\ \omega_{iz} & 0 & -\omega_{ix} \\ -\omega_{iy} & \omega_{ix} & 0 \end{bmatrix} \tag{17}$$

$\mathbf{c}_k\left(\mathbf{x}_k, \dot{\mathbf{x}}_k\right)$ is the centrifugal and Coriolis matrix, is function of the generalized coordinates and velocities $\mathbf{x}_k, \dot{\mathbf{x}}_k$:

$$\mathbf{c}_k\left(\mathbf{x}_k, \dot{\mathbf{x}}_k\right) = \frac{\partial \mathbf{M}_k\left(\mathbf{X}_k\right)}{\partial \mathbf{X}_k}\left(\mathbf{E}_n \otimes \dot{\mathbf{X}}_k\right) - \frac{1}{2}\left(\frac{\partial \mathbf{M}_k\left(\mathbf{X}_k\right)}{\partial \mathbf{X}_k}\left(\dot{\mathbf{X}}_k \otimes \mathbf{E}_n\right)\right)^T \tag{18}$$

Where $\mathbf{E}_n$ is the unit matrix of size [24x24].

$\mathbf{P}_k$ is the [24x1] vector of generalized forces due to potential forces:

$$\mathbf{P}_k\left(\mathbf{X}_k\right) = \left(\frac{\partial \mathbf{\Pi}_k}{\partial \mathbf{X}_k}\right)^T \tag{19}$$

Where $\mathbf{\Pi}_k$ is the potential energy of the system.

$\mathbf{Q}_k$ is the [24x1] vector of generalized forces due to non-conservative forces:

$$\mathbf{Q}_k = \begin{bmatrix} \mathbf{Q}_{k1}, \mathbf{Q}_{k2}, ..., \mathbf{Q}_{k23}, \mathbf{Q}_{k24} \end{bmatrix}^T \tag{20}$$

$\mathbf{U}_k$* is the [1x24] vector whose elements are the generalized forces of the constraint forces at the joints:

$$\mathbf{U}_k = \begin{bmatrix} \mathbf{U}^*_{k1}, \mathbf{U}^*_{k2}, ..., \mathbf{U}^*_{k23}, \mathbf{U}^*_{k24} \end{bmatrix}^T \tag{21}$$

U_k is the [1x24] vector, with elements representing the driving forces at the legs:

$$\mathbf{U}_k = \left[\mathbf{U}_{k1}, \mathbf{U}_{k2}, ...\mathbf{U}_{k6}, 0, 0, 0, ..., 0, 0, 0\right]^T \quad (22)$$

The solution to the dynamic equation system (13) is performed when the dynamic components in the system are computed.

The forward dynamics problem of the robot: Given the driving forces at the legs and external forces acting on the robot, determine the motion of the work plate.

By differentiating the constraint equations twice with respect to time, from (12) we have:

$$\begin{cases} \mathbf{M}_k\left(\mathbf{X}_k\right)\ddot{\mathbf{X}}_k + \mathbf{C}_k\left(\mathbf{X}_k, \dot{\mathbf{X}}_k\right)\dot{\mathbf{X}}_k + \mathbf{P}_k\left(\mathbf{X}_k\right) + \mathbf{Q}_k + \mathbf{U}_k^* &= & \mathbf{U}_k \\ \mathbf{G}_k\left(\mathbf{X}_k\right)\ddot{\mathbf{X}}_k &= & \mathbf{g}_k\left(\mathbf{X}_k, \dot{\mathbf{X}}_k\right) \end{cases} \quad (23)$$

The constraint forces can be expressed in the form of Lagrange multipliers as follows:

$$\mathbf{U}_k^* = \mathbf{G}_k^T \boldsymbol{\lambda}_k \quad (24)$$

$$\text{Where } \mathbf{G}_k = \begin{bmatrix} \dfrac{\partial f_{k1}}{\partial X_{k1}} & ... & \dfrac{\partial f_{k1}}{\partial X_{k24}} \\ ... & ... & ... \\ \dfrac{\partial f_{k18}}{\partial X_{k1}} & ... & \dfrac{\partial f_{k18}}{\partial X_{k24}} \end{bmatrix} \quad (25)$$

Substituting into equation (22) and writing in matrix form, we have:

$$\begin{bmatrix} \mathbf{M}_k\left(\mathbf{X}_k\right) & \mathbf{G}_k^T\left(\mathbf{X}_k\right) \\ \mathbf{G}_k\left(\mathbf{X}_k\right) & 0 \end{bmatrix}\begin{bmatrix} \ddot{\mathbf{X}}_k \\ \boldsymbol{\lambda}_k \end{bmatrix} = \begin{bmatrix} -\mathbf{C}_k\left(\mathbf{X}_k, \dot{\mathbf{X}}_k\right)\dot{\mathbf{X}}_k - \mathbf{P}_k\left(\mathbf{X}_k\right) - \mathbf{Q}_k + \mathbf{U}_k \\ \mathbf{g}_k\left(\mathbf{X}_k, \dot{\mathbf{X}}_k\right) \end{bmatrix} \quad (26)$$

The equations (26) has 42 equations, with 42 unknowns consisting of 24 unknowns for the generalized coordinates, their first and second derivatives, and 18 Lagrange multipliers λ_k.

The inverse dynamics problem: Calculating the inverse dynamics is an important task in controlling the parallel robot system to meet the specified requirements. Given the motion of the work plate $\mathbf{p}_k, \dot{\mathbf{p}}_k, \ddot{\mathbf{p}}_k$ and the external forces $\mathbf{P}_k, \mathbf{Q}_k$ find the motion $\mathbf{q}_k, \dot{\mathbf{q}}_k, \ddot{\mathbf{q}}_k$ and driving forces $\mathbf{U}_k$ at the legs. The motions of the robot legs are solved using the inverse kinematics, where the unknowns in the inverse dynamics include the 6 driving forces variables in $\mathbf{U}_k$ and 18 Lagrange multipliers in $\boldsymbol{\lambda}_k$.

Rewriting the expression $\mathbf{U}_k^* = -\mathbf{G}_k^{*T}\boldsymbol{\lambda}_k$ and substituting it into the first equation of (12), we have:

$$\mathbf{M}_k\left(\mathbf{X}_k\right)\ddot{\mathbf{X}}_k + \mathbf{C}_k\left(\mathbf{X}_k, \dot{\mathbf{X}}_k\right)\dot{\mathbf{X}}_k + \mathbf{P}_k\left(\mathbf{X}_k\right) + \mathbf{Q}_k\left(\mathbf{X}_k\right) = \mathbf{G}_k^{*T}\left(\mathbf{X}_k\right)\boldsymbol{\lambda}_k + \mathbf{U}_k \quad (27)$$

The equations (13) becomes:

$$\begin{cases} \mathbf{M}_k\left(\mathbf{X}_k\right)\ddot{\mathbf{X}}_k + \mathbf{C}_k\left(\mathbf{X}_k, \dot{\mathbf{X}}_k\right)\dot{\mathbf{X}}_k + \mathbf{P}_k\left(\mathbf{X}_k\right) + \mathbf{Q}_k\left(\mathbf{X}_k\right) = \mathbf{K}_k\mathbf{y}_k \\ \mathbf{f}_k\left(\mathbf{X}_k\right) = \mathbf{0} \end{cases} \quad (28)$$

$$\text{Where: } \mathbf{K}_k = \begin{bmatrix} \mathbf{E} & \mathbf{G}_k^{*T} \\ \mathbf{0} & \mathbf{0} \end{bmatrix}_{24x24}; \mathbf{y}_k = \left[U_{k1}, U_{k2}, .., U_{k6}, \lambda_{k1}, \lambda_{k2}, .., \lambda_{k18}\right]^T \quad (29)$$

To compute the inverse dynamic equations (28), the inverse kinematics problem in the second equation is computed first, and then substituted into the first equation to determine the driving forces and Lagrange multipliers, as well as the constraint forces.

Dynamic modeling of the two-stage GSPs

The dynamic equation (13) combined for the two-stage GSPs is written as follows:

$$\begin{cases} \mathbf{M}\left(\mathbf{X}\right)\ddot{\mathbf{X}} + \mathbf{C}\left(\mathbf{X}, \dot{\mathbf{X}}\right)\dot{\mathbf{X}} + \mathbf{P}\left(\mathbf{X}\right) + \mathbf{Q}\left(\mathbf{X}\right) + \mathbf{U}^* = \mathbf{U} \\ \mathbf{f}\left(\mathbf{X}\right) = \mathbf{0} \end{cases} \quad (30)$$

Where:

$$\mathbf{X}_{48x1} = \begin{bmatrix} \mathbf{X}_1 \\ \mathbf{X}_2 \end{bmatrix}; \dot{\mathbf{X}} = \begin{bmatrix} \dot{\mathbf{X}}_1 \\ \dot{\mathbf{X}}_2 \end{bmatrix}; \ddot{\mathbf{X}} = \begin{bmatrix} \ddot{\mathbf{X}}_1 \\ \ddot{\mathbf{X}}_2 \end{bmatrix} \mathbf{M}_{48x48} = \begin{bmatrix} \mathbf{M}_1 \\ \mathbf{M}_2 \end{bmatrix}; \mathbf{C}_{48x48} = \begin{bmatrix} \mathbf{C}_1 \\ \mathbf{C}_2 \end{bmatrix}; \mathbf{P}_{48x1} = \begin{bmatrix} \mathbf{P}_1 \\ \mathbf{P}_2 \end{bmatrix};$$

$$\mathbf{Q}_{48x1} = \begin{bmatrix} \mathbf{Q}_1 \\ \mathbf{Q}_2 \end{bmatrix}; \mathbf{U}_{48x1}^* = \begin{bmatrix} \mathbf{U}_1^* \\ \mathbf{U}_2^* \end{bmatrix}; \mathbf{U}_{48x1} = \begin{bmatrix} \mathbf{U}_1 \\ \mathbf{U}_2 \end{bmatrix}; \mathbf{f}_{36x1}\left(\mathbf{X}\right) = \begin{bmatrix} \mathbf{f}_1\left(\mathbf{X}_1\right) \\ \mathbf{f}_2\left(\mathbf{X}_2\right) \end{bmatrix} \quad (31)$$

The equations of motion (30) has 84 equations, with 84 unknowns consisting of 48 unknowns for the generalized coordinates, their first and second derivatives, and 36 Lagrange multipliers λ.

To design the computed torque controller in the task space, the dynamic equations should be simplified into a compact form that represents the relationship between the driving force at the legs and the variables in the task space. This requires eliminating the Lagrange multipliers, following the method presented in [14]. As previously, the equations are first simplified for a single platform, then extended to the entire system for clarity in the derivation.

From (9), we have:

$$\dot{\mathbf{X}}_k = \begin{bmatrix} \dot{\mathbf{q}}_k \\ \dot{\mathbf{p}}_k \end{bmatrix} = \begin{bmatrix} \mathbf{J}_{qk}^{-1}\mathbf{J}_{pk} \\ \mathbf{E} \end{bmatrix}\dot{\mathbf{p}}_k = \mathbf{H}_k\dot{\mathbf{p}}_k \tag{32}$$

Where $\mathbf{E}_{6x6}$ is the unit matrix.

From equations (12) and (32), we obtain:

$$\ddot{\mathbf{q}}_k = \mathbf{J}_{qk}^{-1}\mathbf{J}_{pk}\ddot{\mathbf{p}}_k + \mathbf{J}_{qk}^{-1}\dot{\mathbf{J}}_{pk}\dot{\mathbf{p}}_k - \mathbf{J}_{qk}^{-1}\dot{\mathbf{J}}_{qk}\mathbf{J}_{qk}^{-1}\mathbf{J}_{pk}\dot{\mathbf{p}}_k \tag{33}$$

Equation (33) can be rewritten in the form:

$$\ddot{\mathbf{X}}_k = \begin{bmatrix} \ddot{\mathbf{q}}_k \\ \ddot{\mathbf{p}}_k \end{bmatrix} = \begin{bmatrix} \mathbf{J}_{qk}^{-1}\mathbf{J}_{pk} \\ \mathbf{E} \end{bmatrix}\ddot{\mathbf{p}}_k + \begin{bmatrix} \mathbf{J}_{qk}^{-1}\dot{\mathbf{J}}_{pk} - \mathbf{J}_{qk}^{-1}\dot{\mathbf{J}}_{qk}\mathbf{J}_{qk}^{-1}\mathbf{J}_{pk} \\ \mathbf{E} \end{bmatrix}\dot{\mathbf{p}}_k = \mathbf{H}_k\ddot{\mathbf{p}}_k + \mathbf{S}_k\dot{\mathbf{p}}_k \tag{34}$$

Multiply both sides of the first equation of (13) by:

$$\mathbf{H}_k^T\mathbf{M}_k\ddot{\mathbf{X}}_k + \mathbf{H}_k^T\mathbf{C}_k\dot{\mathbf{X}}_k + \mathbf{H}_k^T\mathbf{P}_k + \mathbf{H}_k^T\mathbf{Q}_k + \mathbf{H}_k^T\mathbf{G}_k^T\lambda_k = \mathbf{H}_k^T\mathbf{U}_k \tag{35}$$

Since $\mathbf{H}_k\mathbf{G}_k^T\lambda_k = 0$ [14], equation (35) becomes:

$$\mathbf{H}_k^T\mathbf{M}_k\ddot{\mathbf{X}}_k + \mathbf{H}_k^T\mathbf{C}_k\dot{\mathbf{X}}_k + \mathbf{H}_k^T\mathbf{P}_k + \mathbf{H}_k^T\mathbf{Q}_k = \mathbf{H}_k^T\mathbf{U}_k \tag{36}$$

Substitute (9) and (33) into (36):

$$\mathbf{H}_k^T\mathbf{M}_k\mathbf{H}_k\ddot{\mathbf{p}}_k + (\mathbf{H}_k^T\mathbf{M}_k\mathbf{S}_k + \mathbf{H}_k^T\mathbf{C}_k\mathbf{H}_k)\dot{\mathbf{p}}_k + \mathbf{H}_k^T\mathbf{P}_k(\mathbf{X}_k) + \mathbf{H}_k^T\mathbf{Q}_k(\mathbf{X}_k) = \mathbf{H}_k^T\mathbf{U}_k \tag{37}$$

Equation (37) simplifies to:

$$\mathbf{T}_k = \overline{\mathbf{M}}_k\ddot{\mathbf{p}}_k + \overline{\mathbf{C}}_k\dot{\mathbf{p}}_k + \overline{\mathbf{P}}_k + \overline{\mathbf{Q}}_k \tag{38}$$

Where:

$$\overline{\mathbf{M}}_k = \mathbf{H}_k^T\mathbf{M}_k\mathbf{H}_k \,;\; \overline{\mathbf{C}}_k = (\mathbf{H}_k^T\mathbf{M}_k\mathbf{S}_k + \mathbf{H}_k^T\mathbf{C}_k\mathbf{H}_k) \,;\; \overline{\mathbf{P}}_k = \mathbf{H}_k^T\mathbf{P}_k \,;\; \overline{\mathbf{Q}}_k = \mathbf{H}_k^T\mathbf{Q}_k \,;\; \mathbf{T}_k = \mathbf{H}_k^T\mathbf{U}_k \tag{39}$$

III. COMPUTED TORQUE CONTROL IN TASK SPACE

From (38), choose the computed torque control law [15, 16]:

$$\mathbf{T}_k = \overline{\mathbf{M}}_k(\ddot{\mathbf{p}}_{kd} + \mathbf{K}_{kP}\mathbf{e}_k + \mathbf{K}_{kD}\dot{\mathbf{e}}_k) + \overline{\mathbf{C}}_k\dot{\mathbf{p}}_k + \overline{\mathbf{P}}_k + \overline{\mathbf{Q}}_k \tag{40}$$

$\mathbf{e}_k, \dot{\mathbf{e}}_k, \ddot{\mathbf{e}}_k$ are the error vectors for position, orientation, velocity, and acceleration of the work plate of k-th platform, respectively.

$$\mathbf{e}_k = \mathbf{p}_{kd} - \mathbf{p}_k = \begin{bmatrix} e_{k1}, e_{k2}, ..., e_{k6} \end{bmatrix}^T \,;\; \dot{\mathbf{e}}_k = \dot{\mathbf{p}}_{kd} - \dot{\mathbf{p}}_k = \begin{bmatrix} \dot{e}_{k1}, \dot{e}_{k2}, ..., \dot{e}_{k6} \end{bmatrix}^T \tag{41}$$

[15, 16] presents methods for proving system stability.

$\overline{\mathbf{K}}_{kD}, \overline{\mathbf{K}}_{kP}$ are diagonal and positive definite matrices.

$$\overline{\mathbf{K}}_{kP} = diag(K_{kP1}, K_{kP2}, ..., K_{kPs}), K_{kPs} > 0; \overline{\mathbf{K}}_{kD} = diag(K_{kD1}, K_{kD2}, ..., K_{kDs}), K_{kDs} > 0, \; s = 1, 2, ...6 \tag{42}$$

The above expressions for a single platform are combined to expressions for two-stage GSPs as follows:

$$\mathbf{T} = \overline{\mathbf{M}}\ddot{\mathbf{p}} + \overline{\mathbf{C}}\dot{\mathbf{p}} + \overline{\mathbf{P}} + \overline{\mathbf{Q}} \tag{43}$$

The above expressions for a single platform are combined to expressions for two-stage GSPs as follows:

$$\mathbf{T}_{12x1} = \begin{bmatrix} \mathbf{T}_1 \\ \mathbf{T}_2 \end{bmatrix} \,;\; \dot{\mathbf{X}} = \begin{bmatrix} \dot{\mathbf{X}}_1 \\ \dot{\mathbf{X}}_2 \end{bmatrix} \,;\; \ddot{\mathbf{p}} = \begin{bmatrix} \ddot{\mathbf{p}}_1 \\ \ddot{\mathbf{p}}_2 \end{bmatrix} \,;\; \overline{\mathbf{M}}_{12x12} = \begin{bmatrix} \overline{\mathbf{M}}_1 \\ \overline{\mathbf{M}}_2 \end{bmatrix} \,;\; \overline{\mathbf{C}}_{12x12} = \begin{bmatrix} \overline{\mathbf{C}}_1 \\ \overline{\mathbf{C}}_2 \end{bmatrix} \,;\; \overline{\mathbf{P}}_{12x1} = \begin{bmatrix} \overline{\mathbf{P}}_1 \\ \overline{\mathbf{P}}_2 \end{bmatrix} \,;\; \overline{\mathbf{Q}}_{12x1} = \begin{bmatrix} \overline{\mathbf{Q}}_1 \\ \overline{\mathbf{Q}}_2 \end{bmatrix} \,;\; \tag{44}$$

$$\overline{\mathbf{K}}_{P12x1} = \begin{bmatrix} \overline{\mathbf{K}}_{1P} \\ \overline{\mathbf{K}}_{2P} \end{bmatrix} \,;\; \overline{\mathbf{K}}_{D12x1} = \begin{bmatrix} \overline{\mathbf{K}}_{1D} \\ \overline{\mathbf{K}}_{2D} \end{bmatrix} \,;\; \mathbf{e}_{12x1} = \begin{bmatrix} \mathbf{e}_1 \\ \mathbf{e}_2 \end{bmatrix} \,;\; \dot{\mathbf{e}}_{12x1} = \begin{bmatrix} \ddot{\mathbf{e}}_1 \\ \dot{\mathbf{e}}_2 \end{bmatrix} \,;\; \ddot{\mathbf{e}}_{12x1} = \begin{bmatrix} \ddot{\mathbf{e}}_1 \\ \ddot{\mathbf{e}}_2 \end{bmatrix} \tag{45}$$

The computed torque control law of two-stage GSPs:

$$\mathbf{T} = \overline{\mathbf{M}}_{(\mathbf{q})}(\ddot{\mathbf{p}}_d + \mathbf{K}_P\mathbf{e} + \mathbf{K}_D\dot{\mathbf{e}}) + \overline{\mathbf{C}}(\mathbf{q}, \dot{\mathbf{q}})\dot{\mathbf{p}} + \overline{\mathbf{P}}(\mathbf{q}) + \overline{\mathbf{Q}}(\mathbf{q}, \dot{\mathbf{q}}) \tag{46}$$

Figure 4 presents the block scheme of computed torque control in task space of the two-stage GSPs. In the control system diagram, the position and velocity of the work plates are measured using MRU-PD Motion Reference Units from Inertial Labs, which are placed on the work plates of the lower and upper platforms.
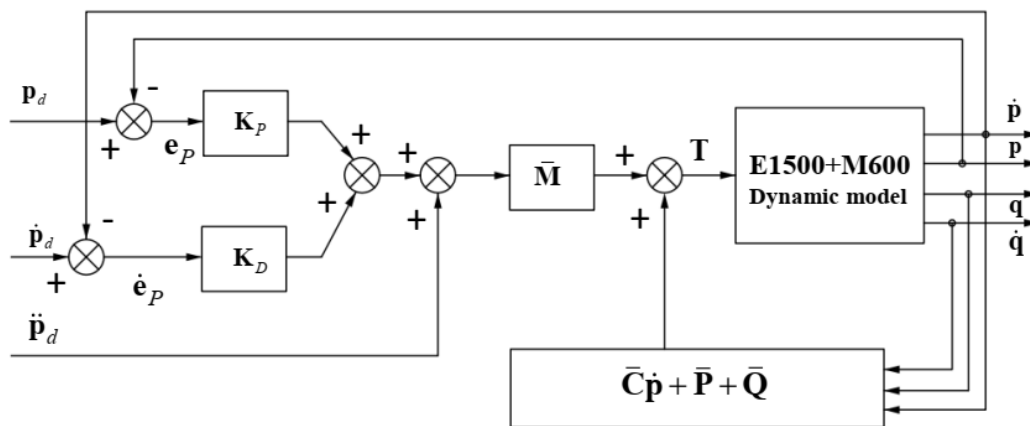
Fig. 3. Block scheme of computed torque control in task space

IV. KINEMATIC AND DYNAMIC PARAMETERS OF THE ROBOT

The platforms used for computations and simulations include: the GSP at stage 1 is eMotion-1500/2700-6DOF-650-MK1 (referred to as E1500), and the GSP at stage 2 is the MicroMotion 600 (referred to as M600) from Bosch Rexroth, Figure 1. The kinematic and dynamic parameters of the lower and upper platform are shown in Table 1 and Table 2. The moments of inertia in Table 2 are calculated relative to the coordinate frame attached to the center of mass of each corresponding rigid body. The center of mass coordinates are calculated relative to the coordinate frame attached to the local frame, as shown in Figure 2.

Table 1. Kinematic parameters of two-stage GSPs

r_{1b} (m)	r_{1p} (m)	σ_{1b} (deg)	σ_{1p} (deg)	r_{2b} (m)	r_{2p} (m)	σ_{2b} (deg)	σ_{2p} (deg)
1.28	1.10	8.60	20.86	0.35	0.32	14.61	21.56

Table 2. Dynamic parameters of two-stage GSPs

	m (kg)	x_C (m)	y_C (m)	z_C (m)	Ixx (kgm2)	Iyy (kgm2)	Izz (kgm2)
Cross B_{1i}	2.46	0	0	0	0.0046	0.0035	0.0035
Cyl B_{1i}	150.4	0	0.059	0.544	19.384	18.392	1.539
Pis P_{1i}	31.63	0	0	-0.375	2.632	2.362	0.046
Cross B_{1i}	2.46	0	0	0	0.0046	0.0035	0.0035
Plate P_1	238.2	0	0	0.150	63.384	63.384	135.562
Cross B_{2i}	0.48	0	0	0	3.56e-5	1.18e-5	1.18e-5
Cyl B_{2i}	9.65	0	0	0.168	0.110	0.110	0.006
Pis P_{2i}	3.84	0	0	-0.144	0.020	0.020	0.0008
Cross P_{2i}	0.48	0	0	0	3.56e-5	1.18e-5	1.18e-5
Plate P_2	36.50	0	0	0.120	1.305	1.305	2.566

Leg lengths of the E1500 platform: stroke length: 950 mm; minimum leg length: 1306.14 mm; maximum leg length: 2256.14 mm. Leg lengths of the M600 platform: stroke length 350 mm; minimum leg length: 463.6 mm; maximum leg length: 813.6 mm.

Figure 5 shows the diagram created in MATLAB/Simulink in combination with MSCAdams software to compute and simulate the motions of the robot system.

V. COMPUTATION AND SIMULATION RESULT

The computed torque controller in the task space is applied to the two-stage platform in the study that the lower platform simulates the oscillations, while the upper platform maintains stable balance.

The PD block of E1500 platform is modified with $K_{1Pi}=5000$, $K_{1Di}=250$ (i=1..6) and the PD block of M600 platform is modified with $K_{2Pi}=5000$, $K_{2Di}=250$ (i=1..6).
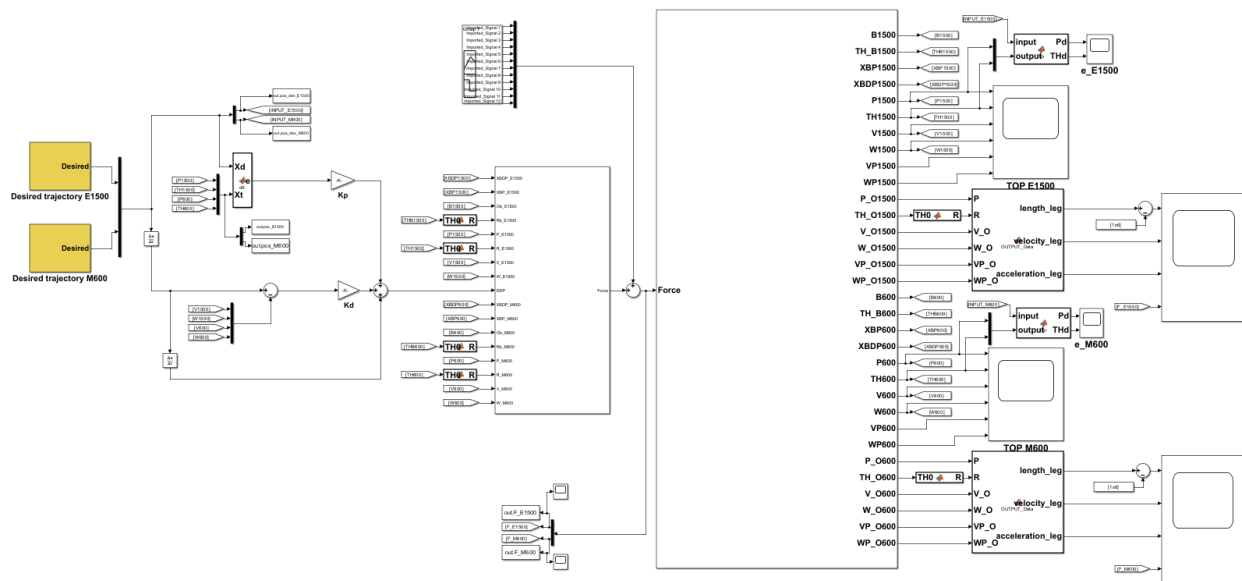
Fig. 5. Robot system diagram in MATLAB/Simulink and MSCAdams

The inputs of the work plates:

The oscillation generated at the work plate of the E1500 simulates the ship's oscillation on sea waves at sea state 6, presented in [17], Figure 6. The motion data of the ship is took from [18], sea state 6, wave type (beta): long-crested (unidirectional), wave coming from bow (front), wave angle: 180 degrees. Ship: HMS Norfolk, dimensions: 137 x15x16m.

The set balance position and orientation of the work plate of the M600 platform:

$$\mathbf{r}_{P2} = \begin{bmatrix} 0 & 0 & 2.403 & 0 & 0 & 0 \end{bmatrix} \tag{46}$$

In this case, input data of the orientation and position of the lower work plate are in numerical form, velocity is calculated using numerical differentiation.
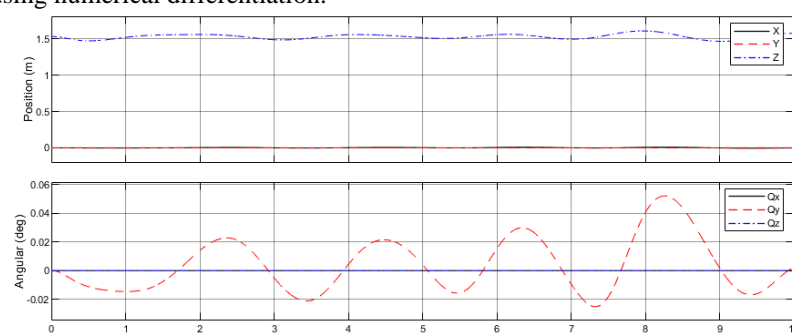
Fig. 6. Oscillations of the ship at sea state 6, wave long-crested [18]

With the oscillations of the work plate on the E1500 are regenerated in Figure 7, the computation program produces results for position, orientation errors, the motion and driving forces of the legs of the E1500 platform, as shown in Figure 8, 9. The set balance position and orientation of the work plate of the M600 (Figure 10), the errors, motion and driving forces of the legs of the M600 platform, as shown in Figure 11, 12.
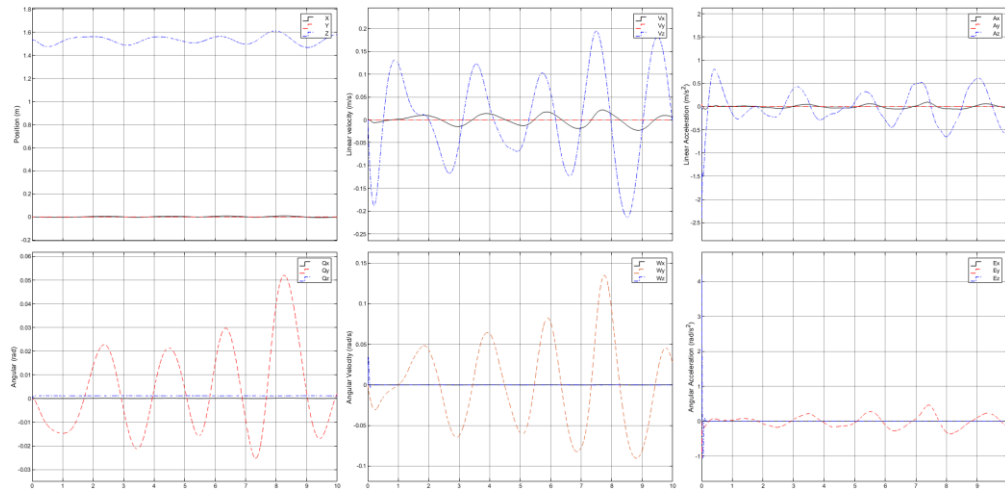
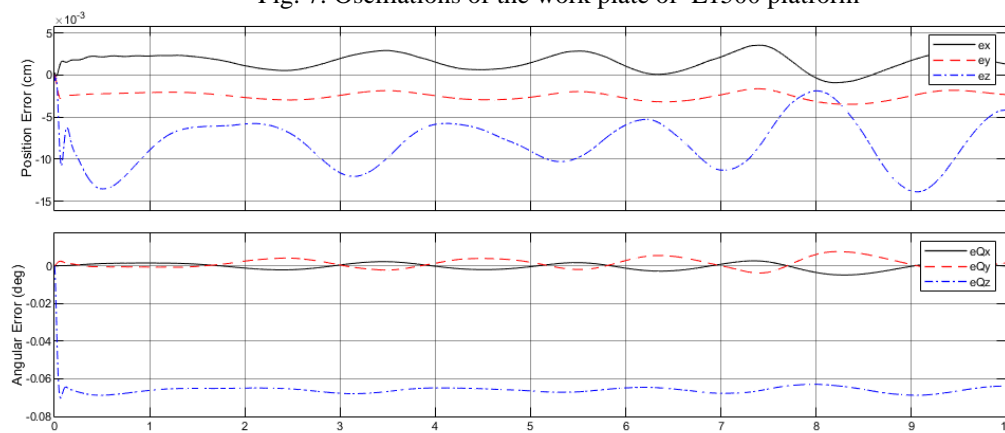Fig. 7. Oscillations of the work plate of E1500 platform

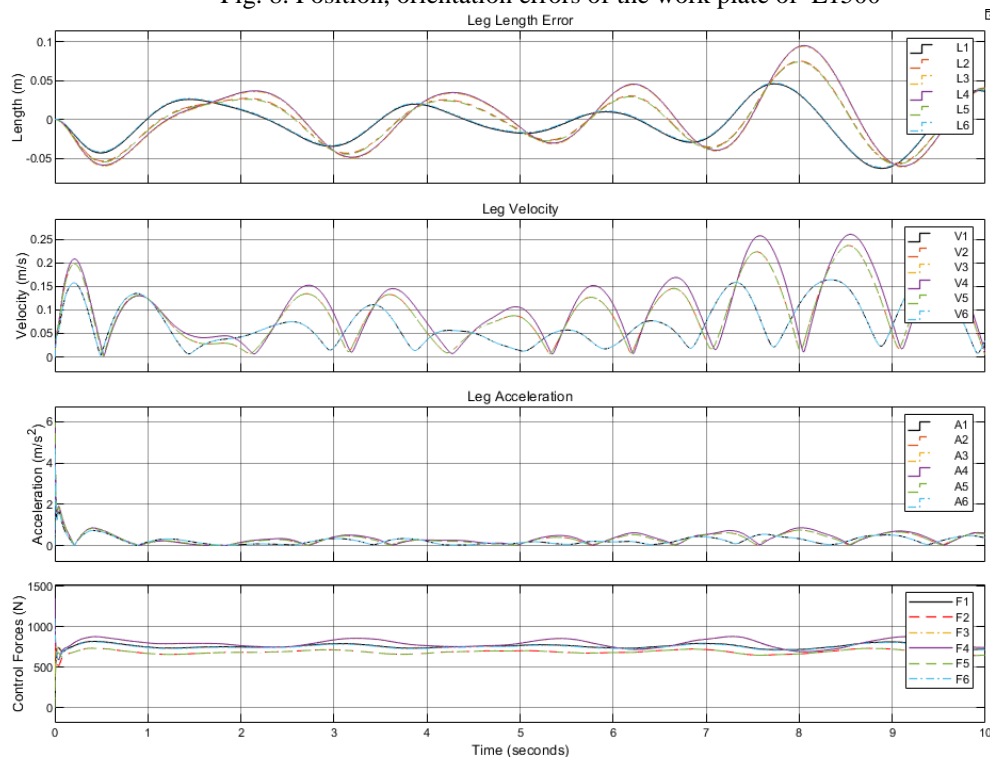Fig. 8. Position, orientation errors of the work plate of E1500

Fig. 9. Position, velocity, acceleration, and forces of the legs of E1500

Simulation results for the E1500 platform: Absolute average position error: 0.0089 cm. Absolute average orientation error: 0.0659 deg. Maximum absolute position error: 0.0142 cm. Maximum absolute orientation error: 0.0703 deg. Maximum control force response: 1353.6270 N
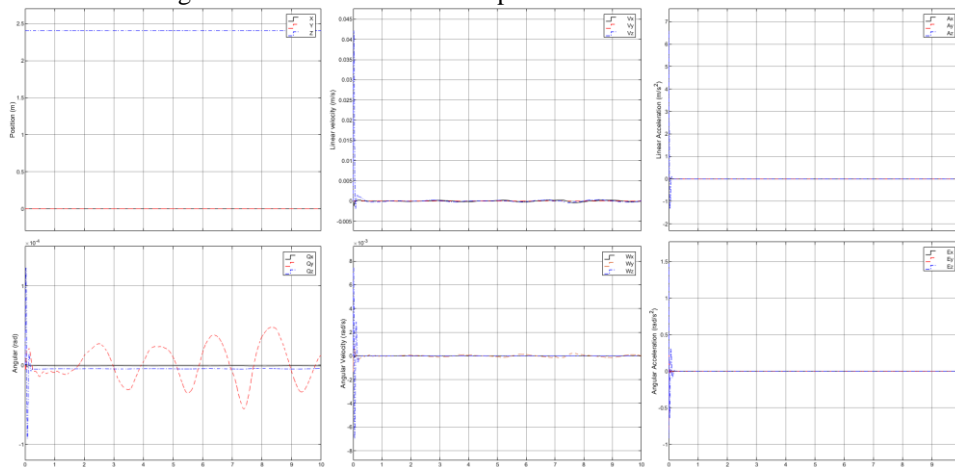
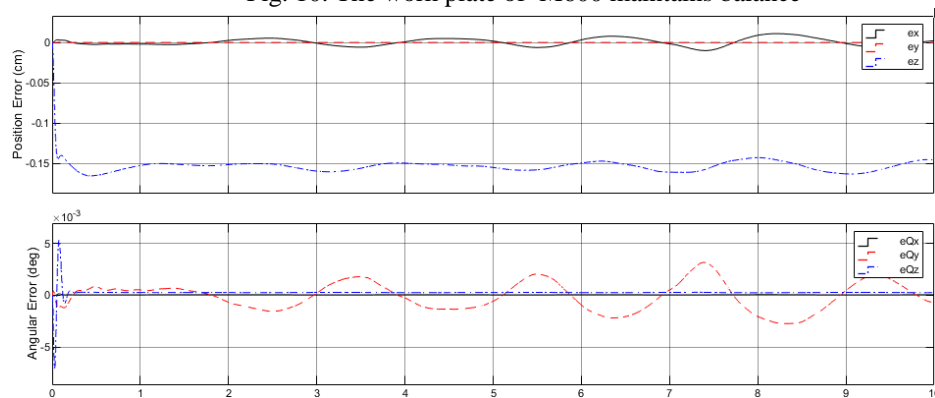Fig. 10. The work plate of M600 maintains balance
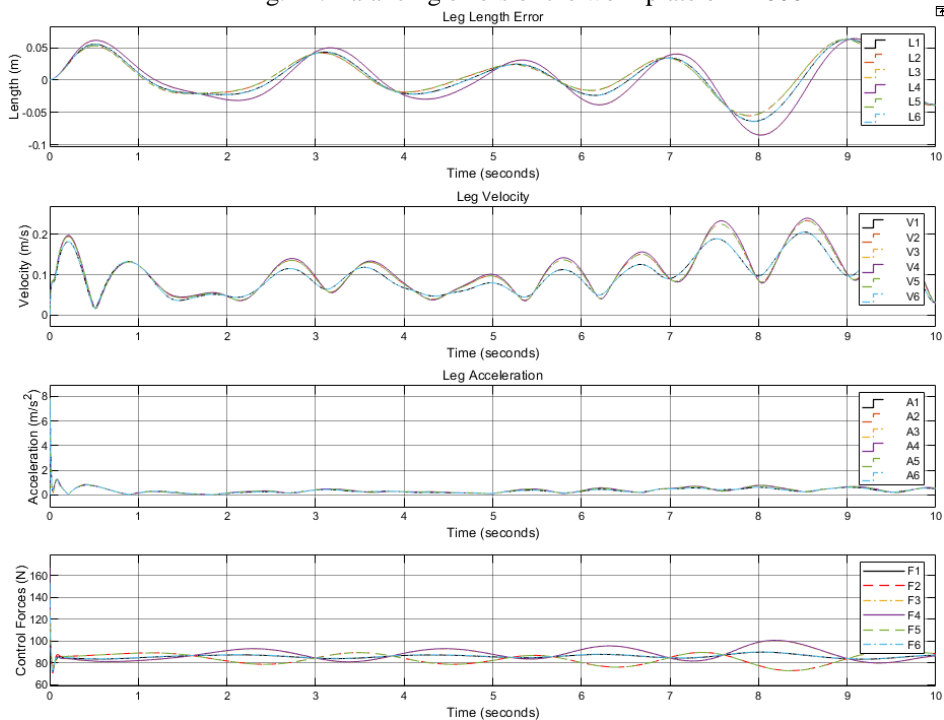
Fig. 11. Balancing errors of the work plate of M600

Fig. 12. Position, velocity, acceleration, and forces of the legs of M600

Simulation results for the M600 platform: Absolute average position error: 0.1532 cm. Absolute average orientation error: 0.0012 deg. Maximum absolute position error: 0.1652 cm. Maximum absolute orientation error: 0.0070 deg. Maximum control force response: 167.3197 N.

VI. CONCLUSION

The computational and simulation outcomes show that the first platform successfully regenerates the required oscillations of the ship, with real-time calculations of its leg motions and driving forces. Meanwhile, the work plate of the second platform achieves stable balance around the desired position with minimal error, making it ideal for balance stabilization in maritime transportation applications.

This study develops kinematic and dynamic model of two-stage Gough-Stewart platform featuring a closed-loop structure and numerous degrees of freedom. The kinematic and dynamic equations establish the relationship between driving forces, constraint forces, external forces, and the movements of the legs and work plates across different stages, facilitating both forward and inverse dynamics analysis.

The designed computed torque controller enables the lower platform to generate vehicle motion oscillations while ensuring stability on the work plate of upper platform.

REFERENCES

[1].   D. Stewart, 1965, A platform with six degrees of freedom, Proceedings of the UK Institute of Mechanical Engineering, 180(1):371–386.
[2].   Ampelmann. www.ampelmann.nl
[3].   Nguyen Thanh Son, Hoang Quang Chinh, Nguyen Dinh Quan, 2017, Investigation on offshore access stabilization Systems-Simulation using the blockset SimMechanics in Matlab/Simulink, J. of Science and Technique, Le Quy Don Technical University, Vol. 183, pp. 88-100.
[4].   Marques, Filipe, et al, 2021, Examination and comparison of different methods to model closed loop kinematic chains using Lagrangian formulation with cut joint, clearance joint constraint and elastic joint approaches, Mechanism and Machine Theory 160: 104294.
[5].   Staicu, Stefan, 2011, Dynamics of the 6-6 Stewart parallel manipulator, Robotics and Computer Integrated Manufacturing 27.1: 212-220
[6].   Abdellatif, H. & Heimann, B., 2009, Computational efficient inverse dynamics of 6-DOF fully parallel manipulators by using the Lagrangian formalism, Mechanism and Machine Theory, 44, pp. 192-207.
[7].   Yang, C., Han, J., Peter, O. O., & Huang, Q. ,2011, PID control with gravity compensation for hydraulic 6-DOF parallel manipulator, PID Control, Implementation and Tuning, doi:10.5772/16023.
[8].   Cai, Yunfei, et al, 2020, Model analysis and modified control method of ship-mounted Stewart platforms for wave compensation, IEEE Access 9: 4505-4517.
[9].   Valente, Vítor Tumelero, and Eduardo André Perondi, 2017, Control of an electrohydraulic Stewart platform manipulator for off-shore motion compensation, Proceedings of the 3rd International Conference on Mechatronics and Robotics Engineering
[10].   Tourajizadeh, Hami, and S. Manteghi, 2016, Design and optimal control of dual-stage Stewart platform using Feedback-Linearized Quadratic Regulator, Advanced Robotics 30.20: 1305-1321.
[11].   Phan Bui Khoi, 2010, Algorithm and Program for Dynamics Calculation of Parallel Robots, Journal of Science and Technology, 48(1), pp. 33-44.
[12].   Phan Bui Khoi, 2005, Investigation inverse kinematics of parallel mechanisms in series connection, Proceedings of The 5th Asian symposium on Applied Electromagnatics and Mechanics, Hanoi, Vietnam, pp. 224-231. (In Vietnamese).
[13].   Phan Bui Khoi, 2010, Algorithm and Program for Dynamics Calculation of Parallel Robots, Journal of Science and Technology, 48(1), pp. 33-44.
[14].   Phan Bui Khoi, Ha Huy Hung, Hoang Quang Chinh, 2024, Algorithm and program for computing the kinematics of a two-stage parallel robot, Proceedings of the National Mechanics Conference, Vol. 2, pp. 705-714. (In Vietnamese).
[15].   Vlase, S, 1987, A method of eliminating Lagrangian multipliers from the equation of motion of interconnected mechanical systems, 235-237.
[16].   Sciavicco, Lorenzo, and Bruno Siciliano, 2012, Modelling and control of robot manipulators, Springer Science & Business Media.
[17].   W., Khalil, E., Dombre: Modeling, Identification and Control of Robots. Kogan page Science Paper Edition (2002).
[18].   Ha Huy Hung, Hoang Quang Chinh, at al, 2022, Simulation of Vessel Oscillation Using Parallel Robot, Journal of Military Science and Technology, No. 80, June 2022, pp. 156-67, doi:10.54939/1859-1043.j.mst.80.2022.156-167. (In Vietnamese)
[19].   https://github.com/LINK-SIC-2021-Bernat-Granstrom/ship-simulator.
[20].   MicroMotion-600 Motion System. www.boschrexroth.com
[21].   Inertial Labs Motion Reference Unit MRU-PD. https://inertiallabs.com/products/mru/
[22].   Dinh-Quan Nguyen, Ha Huy Hung. "Design and Control of a hybrid 2-DOF Balancing Table System". American Journal of Engineering Research (AJER). Volume-9, Issue-8, pp-26-33, 2020.